

Molecular Aggregation Behavior of Perylene-Bridged Bis(β -cyclodextrin) and Its Electronic Interactions upon Selective Binding with Aromatic Guests

Ke-Rang Wang, Dong-Sheng Guo, Bang-Ping Jiang, Zhan-Hu Sun, and Yu Liu*

Department of Chemistry, State Key Laboratory of Elemento-Organic Chemistry, Nankai University, Tianjin 300071, People's Republic of China

Received: September 9, 2009; Revised Manuscript Received: September 27, 2009

A novel water-soluble perylene bisimide derivative **1** was synthesized with two permethyl- β -cyclodextrin grafts at the imide nitrogens, and its structure was identified by NMR, Fourier transform infrared spectroscopy (FT-IR), matrix-assisted laser desorption ionization mass spectrometry (MALDI-MS), and elemental analysis. Its aggregation behavior in water and organic solutions was further investigated by UV-vis, fluorescence, and ^1H NMR spectra, showing that **1** exhibits strong $\pi\cdots\pi$ aggregation in water. Especially, the aggregation and optical properties were comprehensively compared between the neutral form **1** and protonated form **1H₂** through concentration- and temperature-dependent UV-vis experiments. The aggregation constant of **1H₂** is almost 1 order of magnitude lower than that of **1** owing to electrostatic repulsion. On the other hand, **1H₂** exhibits better fluorescence than **1** by overcoming the photoinduced electron transfer process from imino groups to perylene backbone. Furthermore, by employing the binding sites of grafted cyclodextrins to aromatic guests, pronounced electronic interactions between perylene and anthracene/pyrene guests were observed.

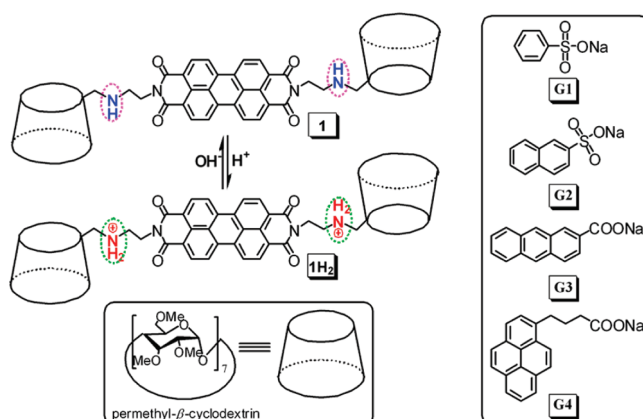
Introduction

In recent years, building well-defined nanosupramolecular objects from extended aromatic building blocks has been one fascinating topic of interdisciplinary research in chemistry, biology, and materials science, which is expected to yield new nanoscale materials with unique electron and photonic properties benefiting from the excitonic interactions between adjacent aromatic units.¹ Among such building blocks, perylene bisimides attract our special interest for their strong $\pi\cdots\pi$ stacking and outstanding optoelectronic properties.² Various perylene bisimide derivatives have been employed to construct nanoscopic architectures with definite morphologies,³ which are further explored for application in liquid crystals, organogels, artificial light harvesting systems, and organic photovoltaic devices.²

It is well-known that creating adaptive systems, whose structure and function can be manipulated, is one main challenge in the field of supramolecular chemistry.⁴ However, the reversible control over $\pi\cdots\pi$ aggregation of perylene bisimides has received much less attention to date. Recently, Rybtchinski and co-workers⁵ reported a new type of photofunctional supramolecular fibers, which allowed for assembly/disassembly with chemical reduction/oxidation of perylene bisimides. Moreover, the electronic interactions between perylene and other chromophores linked by host-guest interactions have not been reported to our best knowledge; these interactions are one significant factor in constructing functional nanosupramolecular materials.

Herein, we report the aggregation behavior and optical property of a water-soluble perylene bisimide derivative **1** with two permethyl- β -cyclodextrin grafts, which can be finely tuned by pH (Scheme 1). The covalent conjugates of perylene and supramolecular host compounds have been reported less frequently to date.⁶ The aim of grafting cyclodextrin units is not only to increase water solubility but also to further extend the

SCHEME 1: Structural Illustration and Ionization Behavior of **1** and **1H₂** and Molecular Structures of Aromatic Guests **G1–G4**



applications of perylene family. Cyclodextrins, a class of cyclic oligosaccharides with 6–8 D-glucose units linked by α -1,4-glucose bonds, have been extensively investigated in molecular recognition⁷ and self-assembly with various well-defined nanostructures.^{7,8} By virtue of both the outstanding optoelectronic properties of perylene bisimides and inclusion performance of cyclodextrins, the binding behavior of **1** to aromatic guest molecules (**G1**, benzenesulfonic acid sodium salt; **G2**, 2-naphthalenesulfonic acid sodium salt; **G3**, 2-anthracenecarboxylate sodium salt; and **G4**, 1-pyrenebutyric acid sodium salt; Scheme 1) was further investigated, clearly showing electronic interactions between **1** and **G4** (or **G3**).

Results and Discussion

Synthesis. The permethyl- β -cyclodextrin-modified perylene bisimide **1** was synthesized by reaction of 6-ethylenediamino-6-deoxy-permethyl- β -cyclodextrin⁹ with 3,4,9,10-perylenetet-

* Corresponding author: fax (+86)22-2350-3625; e-mail yuliu@nankai.edu.cn.

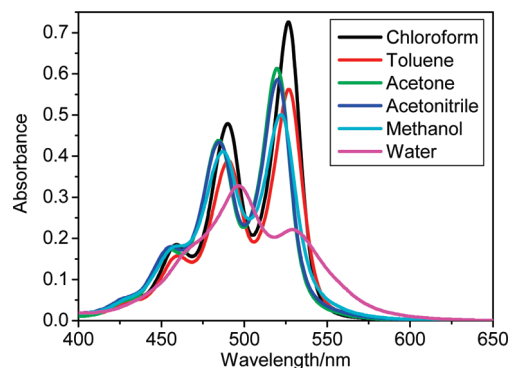


Figure 1. UV-vis spectra of **1** (1.0×10^{-5} M) in different solvents at 25 °C.

racarboxylic dianhydride in the presence of $\text{Zn}(\text{OAc})_2$ as catalyst¹⁰ with a yield of 50%; the product was characterized by NMR, mass spectrometry, and elemental analysis.

Aggregation Behavior in Different Solvents. Benefiting from the grafts of permethyl- β -cyclodextrin, **1** possesses not only liposolubility but also benign water solubility. It allows us to investigate its π -stacking behavior in aqueous solution. UV-vis spectra (Figure 1) show that **1** exists in the typically nonaggregated state in toluene, chloroform, acetonitrile, and acetone and in a very low aggregated state in methanol.¹¹ Three distinguishable absorption bands between 450 and 550 nm are observed, and the most intensity appears at the first band. The well-resolved vibronic structure belongs to the S_0 – S_1 transition of perylene backbone with a transition dipole moment along the long axis of the molecule.¹² The spectrum becomes broader in water, and the maximal absorptivity appears at the second band (497 nm) as a result of excitonic coupling between the adjacent π -stacking perylene bisimides, which indicates the pronounced $\pi \cdots \pi$ aggregation of **1**.¹³ The fluorescence spectra also illuminate the solvent-dependent aggregation behavior that **1** emits much weaker fluorescence in water than in organic solvents (Figure S5 in Supporting Information). These spectral characteristics suggest the strong π -stacking interactions between perylene backbones in water, as the equally nonpolarizable solvents cannot dissolve the π -surfaces well.^{2a}

The aggregation behavior of **1** in different solvents was also identified by ^1H NMR spectroscopy. Perylene protons present a simple pattern of four sharp signals located in the region of 8.70–8.62 ppm in CDCl_3 (Figure S6 in Supporting Information), indicating that **1** exists in the monomeric form (or at most a very low aggregated form) at such a high concentration of 5.0 mM. Whereas in D_2O , perylene shows broad signals (7.91 ppm) and a sharp signal (7.59 ppm), and the protons suffer pronounced upfield shifts because of the π -stacking ring current.¹⁴

The most attractability of **1** is its ionization equilibrium of the imino groups. **1** may assume either the intrinsically neutral form or the protonated dicationic form 1H_2 (Scheme 1). It is reasonably accepted that pH exerts extraordinary influence over the aggregation of **1**, relying on the protonation or not. Moreover, NH group is one kind of typical electron donor that can quench the fluorescence of chromophores via the electron transfer process, and thereby, the optical properties of **1** and its aggregates are also pH-dependent, where the electron transfer can be inhibited by the protonation of NH group.¹⁵

The neutral form **1** exists in the typical nonaggregated state in chloroform according to the aforementioned absorption spectra. When 10 μL of F_3CCOOH is added into 3 mL of chloroform solution, **1** is protonated to 1H_2 , and the absorption bands show a bathochromic shift from 527, 490, and 459 nm

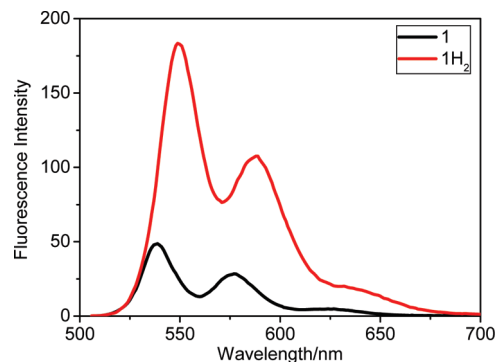


Figure 2. Fluorescence spectra of **1** ($\lambda_{\text{ex}} = 493$ nm, excitation and emission slit width of 2.5 nm, 1.0×10^{-5} M) in chloroform before and after addition of F_3CCOOH at 25 °C.

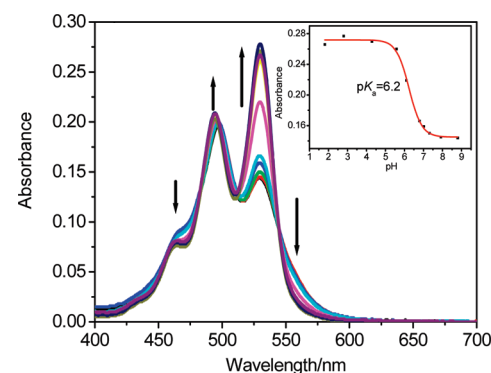


Figure 3. pH-Dependent UV-vis spectra of **1** (5.0×10^{-6} M) in water at 25 °C. (Inset) Variation in absorbance at 529 nm with different pH.

to 534, 497, and 466 nm. The largest absorptivity appears at 534 nm (the first absorption band) (Figure S7 in Supporting Information), which indicates that 1H_2 is also in the nonaggregated state in chloroform.¹² The emission intensity increases nearly 4 times from **1** to 1H_2 (Figure 2). At the initially neutral form, the fluorescence of **1** is quenched by the intramolecular electron transfer (IET) process from the imino groups to perylene. When the imino groups were protonated by F_3CCOOH , the IET process is effectively inhibited in 1H_2 , which leads to the enhancement of fluorescence emission.¹⁵

The pH-dependent absorption and emission spectra were further investigated (pH from 1.8 to 8.8). Decreasing pH values result in the absorptivities of 530 and 497 nm increasing and that of 468 nm decreasing (Figure 3). Especially, the first band (530 nm) increases much more appreciably than the second band (497 nm). It can be seen that the electrostatic repulsion between the protonated imino groups weakens the aggregation capability of perylene bisimide backbones. More pronouncedly, the fluorescence intensity enhances 35 times from **1** to 1H_2 , induced by protonation (Figure S8 in Supporting Information). This increase is assigned to two factors: one is that the IET process cannot occur any more from the protonated imino groups to perylene bisimides,¹⁵ and the other is that the weaker $\pi \cdots \pi$ aggregation takes off the self-quenching effect. By fitting the curves of the pH-dependent absorption and fluorescence changes (eqs 1 and 2), the quantitative pK_a values of **1** were obtained as 6.2 and 6.0, respectively (insets of Figure S8 in Supporting Information).^{15b} Consequently, two pH conditions, pH = 9.0 and 2.0, were selected to compare the aggregation behaviors between the neutral form **1** and the dicationic form 1H_2 .

$$\log [(A_{\max} - A)/(A - A_{\min})] = \text{pH} - \text{p}K_a \quad (1)$$

A_{\max} and A_{\min} are the extrapolated absorbance of the neutral and protonated forms of compound **1**, respectively; A is the observed absorbance at any pH.^{15b}

$$\log [(I_{F_{\max}} - I_F)/(I_F - I_{F_{\min}})] = \text{pH} - \text{p}K_a' \quad (2)$$

$I_{F_{\max}}$ and $I_{F_{\min}}$ are the extrapolated fluorescence intensities of the neutral and protonated forms, respectively; I_F is the observed fluorescence intensity at any pH.^{15b}

Aggregation and Optical Behaviors before and after Protonation. The $\pi \cdots \pi$ aggregation of perylene bisimides is demonstrated to be concentration-dependent.^{2a,16} Absorption spectral changes of **1** as a function of concentration (Figure 4a) show that **1** assumes the aggregation state even at a low concentration of 3.0×10^{-6} M.¹⁴ Both the apparent absorption coefficients of 529 and 496 nm decrease upon increasing concentrations, but with obviously more pronounced variation at 529 nm than 496 nm, and concomitantly, the absorption bands shift slightly from 496 and 529 nm to 498 and 537 nm, which reflects the stronger and stronger electronic coupling between the perylene backbones gone with the enhancement of concentrations. Moreover, the apparent absorption coefficients decrease slightly when the concentration changes from 4.0×10^{-5} M to 1.0×10^{-4} M, indicating that the aggregation leans to equilibrium gradually.^{14d}

The dicationic form **1H₂** is judged as a nonaggregated state or at most a very low aggregated state at the lower concentration of 3.0×10^{-6} M according to the well-resolved vibronic structure observed in the absorption spectrum, and the maximal absorptivity appears at 530 nm.¹² When the concentrations are increased (3.0×10^{-6} M to 1.0×10^{-4} M), the absorption spectral changes of **1H₂** are similar to that of **1**. Utilizing nonlinear least-squares regression analysis of the concentration-dependent UV-vis spectral data by the isodesmic or equal-K model (eq 3; Figure S9 in Supporting Information),¹⁷ the quantitative aggregation constants of **1** and **1H₂** were obtained as 4.7×10^5 M⁻¹ and 5.7×10^4 M⁻¹, respectively. The aggregation ability of **1H₂** is 1 order of magnitude weaker than that of **1** owing to electrostatic repulsion between the positive charges of protonated imino groups. The average dye numbers per stack N (average aggregation number) at different concentrations can then be calculated from the reported equation (eq 4).^{12b} The average aggregation numbers of **1** and **1H₂** are 7 and 3 at 1.0×10^{-4} M, respectively, as illustrated in Figure 6d.

$$\varepsilon(c) = \frac{2Kc + 1 - \sqrt{4Kc + 1}}{2K^2c^2}(\varepsilon_f - \varepsilon_a) + \varepsilon_a \quad (3)$$

ε denotes the apparent extinction coefficient obtained from the spectra; ε_f and ε_a are the extinction coefficients for the free and the aggregated species, respectively; K is the binding constant; and c is the total dye concentration in the sample.¹⁷

$$N = \frac{1}{2}(1 + \sqrt{4Kc + 1}) \quad (4)$$

N is the average aggregation number, K is the aggregation constant, and c is the concentration of the sample.^{12b}

The $\pi \cdots \pi$ aggregation of perylene bisimides is also temperature-dependent,^{2a,16} where the spectral changes are highly

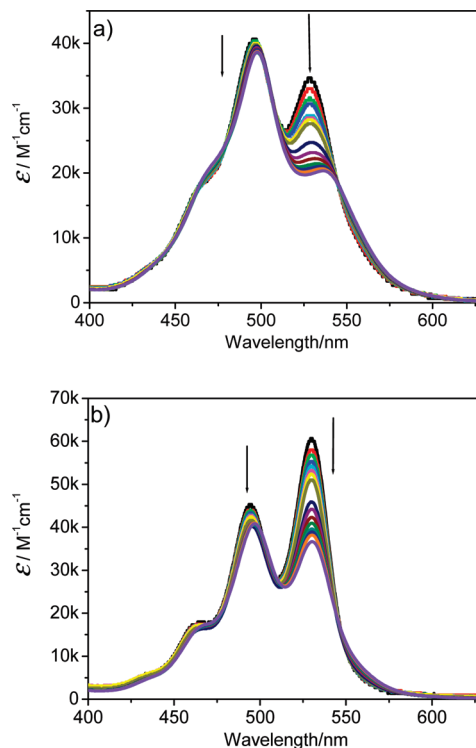


Figure 4. Concentration-dependent UV-vis spectra of (a) **1** (pH = 9.0) and (b) **1H₂** (pH = 2.0) in water at 25 °C; concentrations range from 3.0×10^{-6} M to 1.0×10^{-4} M.

comparable with those observed in concentration-dependent measurements. At 7.0×10^{-5} M, the aggregate of **1H₂** melts gradually when the temperature rises from 5 to 70 °C (Figure S10b in Supporting Information). However, within the same situations, the aggregate of **1** almost maintains its initial state (Figure S10a in Supporting Information), which also indicates the much stronger $\pi \cdots \pi$ stacking interactions for **1** than **1H₂**.

Besides the absorption spectra, the emission spectra of **1** are also pH-dependent as mentioned above. At 1.0×10^{-6} M, **1** and **1H₂** are both prior to monomer state according to the detected aggregation constants, and the corresponding fluorescence quantum yields are 6.3% and 35.5%, respectively. With augmentation of concentrations, the fluorescence intensity is reduced by self-quenching effect upon aggregation. At 1.0×10^{-4} M, **1H₂** exists in a mixture of monomer, dimer, trimer (maybe mainly according to the aggregation constant), etc., and emits yellow color, representing the excimer-state fluorescence with a maximum at 586 nm (Figure 5).^{11b} The fluorescence of **1** at the same concentration can be neglected in comparison with **1H₂**. Therefore, it presents an interesting result that **1** possesses more benign aggregation ability, whereas **1H₂** exhibits much better optical properties (Figure 6d). Both the aggregation behavior and optical property are dominantly controlled by pH, so that the protonation of imino groups can pronouncedly sensitize the fluorescence by inhibiting the electron transfer process and weaken the $\pi \cdots \pi$ stacking interactions owing to the electrostatic repulsion forces.

The aggregation morphologies of **1** and **1H₂** were intuitively distinguished from the TEM and SEM images (Figure 6). **1** shows flakelike aggregates in both TEM and SEM images, with a diameter about 80 nm in the TEM image, while **1H₂** shows small blobs only. This is consistent with the aforementioned results in solution that **1H₂** shows lower aggregation than **1**. Furthermore, the size distributions of aggregates of **1** and **1H₂** were determined by dynamic light scattering (DLS) at the

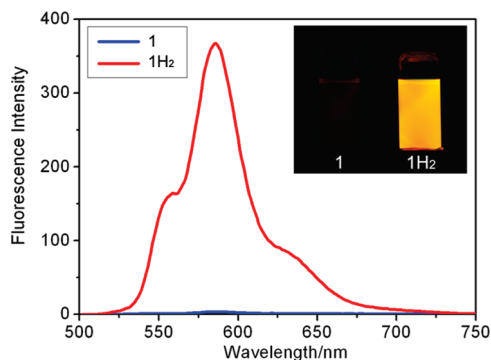


Figure 5. Fluorescence spectra ($\lambda_{\text{ex}} = 465$ nm, excitation slit width of 2.5 nm and emission slit width of 5.0 nm) of **1** and **1H₂** (1.0×10^{-4} M) in water at 25 °C. (Inset) Photographs of **1** and **1H₂** (1.0×10^{-4} M) under UV-light irradiation.

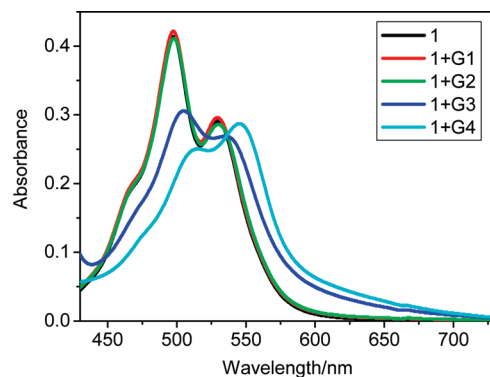


Figure 7. UV-vis spectral changes of **1** (1.0×10^{-5} M) upon addition of 50 equiv of aromatic guest molecules (**G1**, **G2**, **G3**, and **G4**) in phosphate buffer (pH = 8.67, 0.05 M).

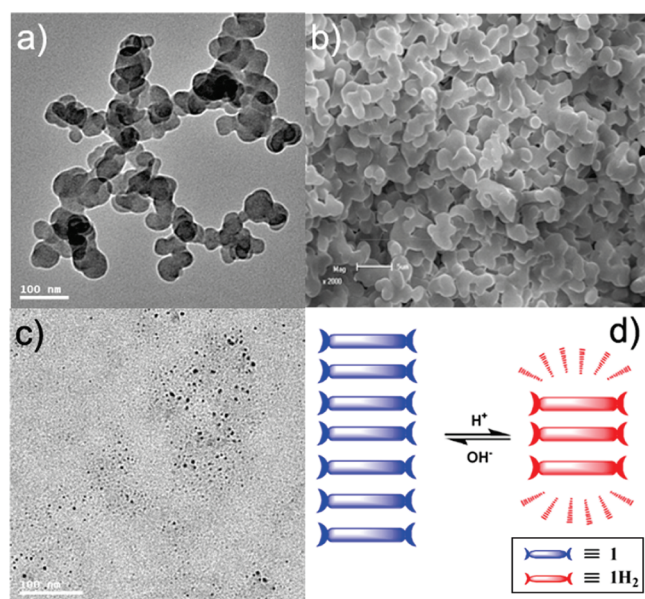


Figure 6. (a) TEM image of **1**; (b) SEM image of **1**; (c) TEM image of **1H₂**, and (d) pH-dependent assembly modes of **1** (blue) and **1H₂** (red) in aqueous solution.

concentration of 1.0×10^{-4} M (Figure S11 in Supporting Information). The mean diameter of aggregate **1** is about 130 nm, which is somewhat larger than that observed in the TEM image because the aggregates shrink without solvents under the conditions of TEM. However, no large aggregation species of **1H₂** were detected by DLS.

Binding Properties for Aromatic Molecules. The $\pi \cdots \pi$ aggregation of perylene bisimides is one of the most promising strategies for the preparation of photofunctional materials, which proves useful for developing insights into organic photovoltaic devices due to the migration of the electron between several close individual stacks. Moreover, these electronic/optoelectronic properties are always affected by the adjacent aromatic groups.¹⁸ Based on the intrinsic inclusion capability of cyclodextrins, the electronic interactions between **1** and a series of aromatic guests (**G1–G4**, Scheme 1) were further examined. As shown in Figure 7, the absorption bands of **1** do not undergo appreciable change upon addition of 50 equiv of **G1** and **G2**, while clearly they undergo a bathochromic shift once **G3** and **G4** are added (pH = 8.67, 0.05 M phosphate buffer).

The apparent binding stoichiometry of **1** with **G3** and **G4** was determined as 1:1 by the Job's plot method, where the plot maximum points appear at a molar fraction of **G3** or **G4** of 0.5

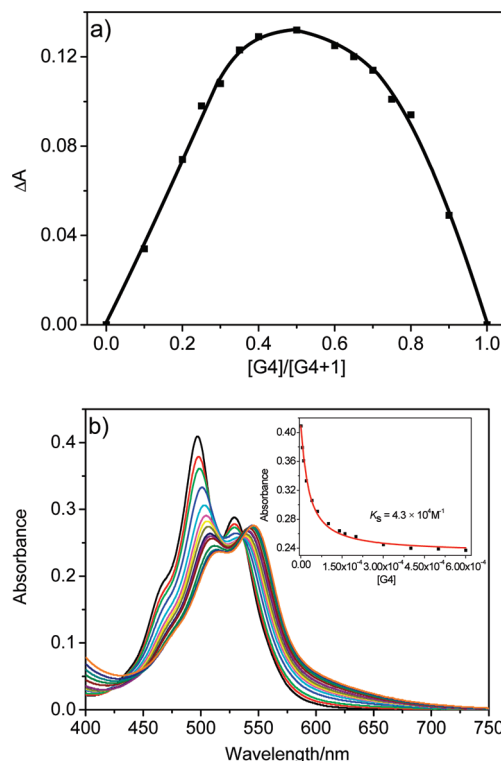


Figure 8. (a) Job's plot for **1** upon complexation with **G4** and (b) UV-vis spectral changes of **1** (1.0×10^{-5} M) upon addition of **G4** in phosphate buffer (pH = 8.67, 0.05 M) at 20 °C. Absorption changes were recorded at 497 nm, and the sum of the total concentrations of hosts and guests is constant (5.0×10^{-5} M). (Inset) Fitting plot of the complexation stability constant for **G4** with **1**.

(Figure 8a; Figure S12a in Supporting Information).¹⁹ Consequently, we obtained the complexation stability constants as $9.1 \times 10^3 \text{ M}^{-1}$ (for **G3**) and $4.3 \times 10^4 \text{ M}^{-1}$ (for **G4**) using the nonlinear least-squares curve-fitting method²⁰ by fitting the experimental data of the second band changes of **1** upon gradual addition of **G3** or **G4** (Figure 8b; Figure S12b in Supporting Information). Meanwhile, other titration curves plotted at different wavelengths were also fitted for **G4** with **1** (Figure S13 in Supporting Information), giving similar constants within acceptable error levels.

The 2D NOESY spectrum of an equimolar mixture of **1** with **G4** (left panel in Figure 9) shows clear NOE cross-peaks between the pyrene protons ($\delta = 7.54\text{--}6.99$ ppm, box A), butyl protons ($\delta = 2.74, 2.14,$ and 1.72 ppm, box B) and the protons of permethyl- β -cyclodextrin, which suggests that **G4** is encapsulated into the cavities of cyclodextrins. In addition, clear NOE

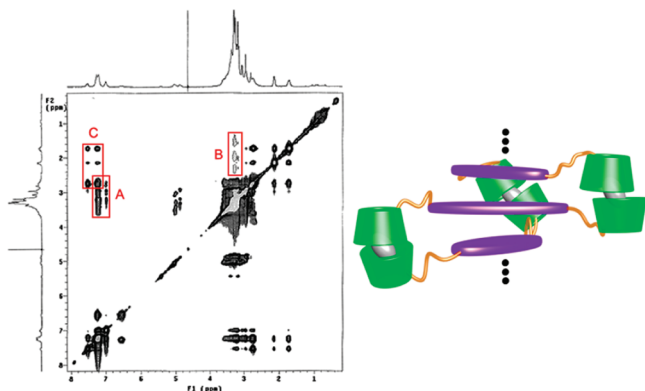


Figure 9. Two-dimensional NOESY spectrum of the equimolar mixture of **1** with **G4** (D_2O , 5.0 mM) and schematic representation of the possible complex formation between **1** and **G4**.

cross-peaks between the pyrene protons and the butyl protons (box C) are observed, indicating that **G4** assumes the contracted conformation with butyl chain close to the pyrene segment. Combining the NMR and aforementioned Job's result, the possible binding geometry between **1** and **G4** was consequently inferred (right panel in Figure 9).

G3 induces the absorption bands of **1** shift from 530 and 497 nm to 537 and 505 nm, and **G4** does to a greater extent, 546 and 514 nm. The bathochromic shifts arise from changes of the relative orientation of the transition dipole moments of the perylene bisimide backbones induced by the electronic interactions between **1** with guests. For **G1** and **G2**, the relatively small conjugate area cannot form appreciable electronic interactions with perylene of **1**, and thereby they cannot influence the orientation of the transition dipole moments. It can also interpret why the electronic interaction of **G4** with **1** is stronger than that of **G3**.

Conclusion

A water-soluble perylene bisimide derivative **1** has been synthesized with two permethyl- β -cyclodextrin grafts at the imide nitrogens, which shows the pH-dependent aggregation behavior and fluorescence property. **1** shows much stronger $\pi \cdots \pi$ stacking interaction in water than the organic solvents. The aggregation ability of **1** in the neutral form is nearly 1 order of magnitude stronger than that of **1H₂** in the protonated form because the electrostatic repulsion between the protonated imino groups plays a certainly unfavorable role in the $\pi \cdots \pi$ stacking of perylene backbones. Nevertheless, both the monomer and oligomer of **1H₂** exhibit several times better fluorescence properties than **1**, resulting from the effective inhibition of the intramolecular electron transfer process from the imino groups to the aromatic perylene backbone. Furthermore, by employing the binding sites of grafted cyclodextrins, the hierarchical self-assembly was performed via including the aromatic guests, showing that pronounced electronic interactions between perylene backbone of **1** and anthracene/pyrene subunits were observed. The interesting optoelectronic and aggregated properties tuning by pH, combined with the elegant inclusion ability of cyclodextrin site, make perylene-bridged bis(β -cyclodextrin) a potential candidate for future applications in optoelectronic devices and also optical sensors.

Experimental Section

Instrumentation. NMR spectra were recorded on a Varian 300 spectrometer. Positive-ion matrix-assisted laser desorption

ionization mass spectrometry was performed on an IonSpec QFT-MALDI MS. Elemental analysis was performed on a Perkin-Elmer-2400C instrument. Fourier transform infrared (FT-IR) spectrum was recorded on a Shimadzu Bio-Rad FTS 135 instrument. UV-vis spectra were recorded on a Shimadzu UV-3600 spectrophotometer equipped with a PTC-348WI temperature controller. Steady-state fluorescence spectra were recorded on a Varian Cary Eclipse equipped with a Varian Cary single-cell peltier accessory to maintain the temperature. The fluorescence quantum yields were recorded on an Edinburgh Analytical Instruments FLS920 spectrometer. The pH values of the solution were adjusted by adding dilute hydrochloric acid or sodium hydroxide solutions, and a PHS-3C instrument (Shanghai Rex Instrument Factory) was used for pH measurement. Transmission electron microscopic (TEM) images were recorded on Philips Tecnai G2 20S-TWIN microscope. Scanning electron microscopic (SEM) images were recorded on a Hitachi S-3500N scanning electron microscope. The dynamic light scattering (DLS) was performed on a laser light scattering spectrometer (BI-200SM) equipped with a digital correlator (BI-9000AT) at 636 nm.

Synthesis of 1. 6-Ethylenediamino-6-deoxypermethyl- β -cyclodextrin was synthesized according to literature procedures from natural β -cyclodextrin.⁹ 6-Ethylenediamino-6-deoxypermethyl- β -cyclodextrin (0.98 g, 0.67 mmol), perylene-3,4,9,10-tetracarboxylic acid bisanhydride (0.13 g, 0.33 mmol), and zinc acetate (0.073 g, 0.33 mmol) were mixed in pyridine (200 mL). The reaction mixture was heated at 100 °C under N_2 for 48 h. After the mixture was cooled to room temperature, the solvent was removed at reduced pressure and the residue was dissolved in chloroform, washed with water, dried over Na_2SO_4 , and evaporated to dryness under vacuum. The residue was purified by silica-gel column chromatography with chloroform-methanol ($v/v = 30/1$) as the eluent to give the product as a red powder (554 mg) with a yield of 50%. FT-IR (KBr) ν [cm^{-1}] 1698, 1661; 1H NMR ($CDCl_3$, 300 MHz, ppm) $\delta = 8.67$ (m, 8 H, Ar-CH), 5.13–5.05 (m, 14 H), 4.36–3.17 (m, 214 H); ^{13}C NMR ($CDCl_3$, 300 MHz, ppm) $\delta = 163.5, 134.8, 131.6, 129.5, 126.7, 123.5, 123.3, 99.1, 99.0, 98.8, 82.3, 82.0, 81.8, 81.4, 80.5, 80.4, 80.3, 80.0, 71.6, 71.1, 61.6, 59.3, 59.1, 58.6, 58.2, 49.5, 48.0, 40.6$; MALDI-MS calcd for $C_{152}H_{236}N_4O_{72}Na^+$, 3292.4821; found 3292.4808. Anal. Calcd for $C_{152}H_{236}N_4O_{72}$: C 55.80, H 7.27, N 1.71. Found: C 55.67, H 7.18, N 1.82.

Acknowledgment. We thank 973 Program (2006CB932900), NNSFC (20703025 and 20721062), and Tianjin Natural Science Foundation (07QTPTJC29600) for financial support.

Supporting Information Available: NMR, FT-IR, and MALDI-MS spectra of **1** and other data as described in the text. This material is available free of charge via the Internet at <http://pubs.acs.org>.

References and Notes

- (1) (a) Ajayaghosh, A.; Praveen, V. K. *Acc. Chem. Res.* **2007**, *40*, 644–656. (b) Grimsdale, A. C.; Müllen, K. *Angew. Chem., Int. Ed.* **2005**, *44*, 5592–5629. (c) Lee, C. C.; Grenier, C.; Meijer, E. W.; Schenning, A. P. H. J. *Chem. Soc. Rev.* **2009**, *38*, 671–683. (d) Ryu, J. H.; Hong, D. J.; Lee, M. *Chem. Commun.* **2008**, 1043–1054.
- (2) (a) Würthner, F. *Chem. Commun.* **2004**, 1564–1579. (b) Elemans, J. A. A. W.; van Hameren, R.; Nolte, R. J. M.; Rowan, A. E. *Adv. Mater.* **2006**, *18*, 1251–1266. (c) Wasielewski, M. R. *J. Org. Chem.* **2006**, *71*, 5051–5066.
- (3) Zang, L.; Che, Y.; Moore, J. S. *Acc. Chem. Res.* **2008**, *41*, 1596–1608.
- (4) (a) Lehn, J. M. *Proc. Natl. Acad. Sci. U.S.A.* **2002**, *99*, 4763–4768. (b) Lehn, J. M. *Chem. Soc. Rev.* **2007**, *36*, 151–160.

- (5) (a) Baram, J.; Shirman, E.; Ben-Shitrit, N.; Ustinov, A.; Weissman, H.; Pinkas, I.; Wolf, S. G.; Rybtchinski, B. *J. Am. Chem. Soc.* **2008**, *130*, 14966–14967. (b) Gebers, J.; Rolland, D.; Frauenrath, H. *Angew. Chem., Int. Ed.* **2009**, *48*, 4480–4483.
- (6) (a) Hippus, C.; Schlosser, F.; Vysotsky, M. O.; Böhmer, V.; Würthner, F. *J. Am. Chem. Soc.* **2006**, *128*, 3870–3871. (b) Hippus, C.; van Stokkum, I. H. M.; Zangrando, E.; Williams, R. M.; Würthner, F. *J. Phys. Chem. C* **2007**, *111*, 13988–13996. (c) Hippus, C.; van Stokkum, I. H. M.; Gsänger, M.; Groeneveld, M. M.; Williams, R. M.; Würthner, F. *J. Phys. Chem. C* **2008**, *112*, 2476–2486. (d) Hippus, C.; van Stokkum, I. H. M.; Zangrando, E.; Williams, R. M.; Wykes, M.; Beljonne, D.; Würthner, F. *J. Phys. Chem. C* **2008**, *112*, 14626–14638. (e) Liu, Y.; Wang, K. R.; Guo, D. S.; Jiang, B. P. *Adv. Funct. Mater.* **2009**, *19*, 2230–2235.
- (7) Liu, Y.; Chen, Y. *Acc. Chem. Res.* **2006**, *39*, 681–691.
- (8) Harada, A. *Acc. Chem. Res.* **2001**, *34*, 456–464.
- (9) (a) Lai, X. H.; Ng, S. C. *Tetrahedron Lett.* **2004**, *45*, 4469–4472. (b) Kang, S.; Chen, Y.; Shi, J.; Ma, Y. H.; Liu, Y. *Chem. J. Chin. Univ.* **2007**, *28*, 458–461.
- (10) Langhals, H. *Chem. Ber.* **1985**, *118*, 4540–4543.
- (11) (a) Zhang, X.; Chen, Z.; Würthner, F. *J. Am. Chem. Soc.* **2007**, *129*, 4886–4887. (b) Schmidt, C. D.; Böttcher, C.; Hirsch, A. *Eur. J. Org. Chem.* **2007**, 5497–5505. (c) Wang, W.; Wan, W.; Zhou, H. H.; Niu, S.; Li, A. D. Q. *J. Am. Chem. Soc.* **2003**, *125*, 5248–5249. (d) Marcon, R. O.; dos Santos, J. G.; Figueiredo, K. M.; Brochsztain, S. *Langmuir* **2006**, *22*, 1680–1687.
- (12) (a) Sadrai, M.; Hadel, L.; Sauers, R. R.; Husain, S.; Krogh-Jespersen, K.; Westbrook, J. D.; Bird, G. R. *J. Phys. Chem.* **1992**, *96*, 7988–7996. (b) Chen, Z.; Stepanenko, V.; Dehm, V.; Prins, P.; Siebbeles, L. D. A.; Seibt, J.; Marquetand, P.; Engel, V.; Würthner, F. *Chem.—Eur. J.* **2007**, *13*, 436–449.
- (13) (a) Seibt, J.; Marquetand, P.; Enge, V.; Chen, Z.; Dehm, V.; Würthner, F. *Chem. Phys.* **2006**, *328*, 354–362. (b) Fink, R. F.; Seibt, J.; Engel, V.; Renz, M.; Kaupp, M.; Lochbrunner, S.; Zhao, H. M.; Pfister, J.; Würthner, F.; Engels, B. *J. Am. Chem. Soc.* **2008**, *130*, 12858–12859.
- (14) (a) Shaller, A. D.; Wang, W.; Gan, H.; Li, A. D. Q. *Angew. Chem., Int. Ed.* **2008**, *47*, 7705–7709. (b) Wang, W.; Han, J. J.; Wang, L. Q.; Li, L. S.; Shaw, W. J.; Li, A. D. Q. *Nano Lett.* **2003**, *3*, 455–458. (c) Wang, W.; Li, L. S.; Helms, G.; Zhou, H. H.; Li, A. D. Q. *J. Am. Chem. Soc.* **2003**, *125*, 1120–1121. (d) Li, A. D. Q.; Wang, W.; Wang, L. Q. *Chem.—Eur. J.* **2003**, *9*, 4594–4601.
- (15) (a) Zang, L.; Liu, R.; Holman, M. W.; Nguyen, K. T.; Adams, D. M. *J. Am. Chem. Soc.* **2002**, *124*, 10640–10641. (b) Daffy, L. M.; de Silva, A. P.; Gunaratne, H. Q. N.; Huber, C.; Lynch, P. L. M.; Werner, T.; Wolfbeis, O. S. *Chem.—Eur. J.* **1998**, *4*, 1810–1815.
- (16) Chen, Z.; Lohr, A.; Saha-Möller, C. R.; Würthner, F. *Chem. Soc. Rev.* **2009**, *38*, 564–584.
- (17) Würthner, F.; Thalacker, C.; Diele, S.; Tschierske, C. *Chem.—Eur. J.* **2001**, *7*, 2245–2253.
- (18) (a) van der Boom, T.; Hayes, R. T.; Zhao, Y.; Bushard, P. J.; Weiss, E. A.; Wasielewski, M. R. *J. Am. Chem. Soc.* **2002**, *124*, 9582–9590. (b) Würthner, F.; Chen, Z.; Hoebein, F. J. M.; Osswald, P.; You, C. C.; Jonkheijm, P. v.; Herrikhuyzen, J.; Schenning, A. P. H. J.; van der Schoot, P. P. A. M.; Meijer, E. W.; Beckers, E. H. A.; Meskers, S. C. J.; Janssen, R. A. J. *J. Am. Chem. Soc.* **2004**, *126*, 10611–10618. (c) Mathew, S.; Johnston, M. R. *Chem.—Eur. J.* **2009**, *15*, 248–253.
- (19) (a) Yang, H.; Bohne, C. *J. Phys. Chem.* **1996**, *100*, 14533–14539. (b) Hollas, M.; Chung, M. A.; Adams, J. *J. Phys. Chem. B* **1998**, *102*, 2947–2953.
- (20) Inoue, Y.; Yamamoto, K.; Wada, T.; Everitt, S.; Gao, X. M.; Hou, Z. J.; Tong, L. H.; Jiang, S. K.; Wu, H. M. *J. Chem. Soc., Perkin Trans. 2* **1998**, 1807–1816.

JP908699B